http://dx.doi.org/10.5755/j01.eee.18.8.2607 ELEKTRONIKA IR ELEKTROTECHNIKA, ISSN 1392-1215, VOL. 18, NO. 8, 2012

Amplitude Noise of Electrical Oscillators Based on the LTV Model

S. A. Hashemi, H. Ghafoorifard, A. Abdipour
Department of Electrical Engineering, Amirkabir University of Technology, 424, Hafez Ave., Tehran, Iran, phone: +98 21 64543327
ahashemi@aut.ac.ir

***Abstract*—In this paper, using the Linear Time Variant (LTV) noise model of oscillators, an analytical expression for Amplitude Impulse Sensitivity Function (A-ISF) based on the limit cycle of the oscillator is derived for the first time. Also Considering the existing expression for Phase Impulse Sensitivity Function (P-ISF), it is shown that P-ISF and A-ISF are correlated. The derived A-ISF is used to simulate the amplitude noise of the oscillators in the $1/f^2$ region of the noise spectrum by the LTV model. Simulation and experimental results show the validity of the derived formula.**

***Index Terms*— Circuit noise, oscillators, phase noise, white noise.**

I. INTRODUCTION

For many years, phase and amplitude noises of electrical oscillators have been the subject of study, and many models have been introduced. The Linear Time Variant Model (LTV) [1], [2] is a formulated and simple model that offers closed form formulas for phase and amplitude noises which include the effect of circuit elements in the output noises. In the LTV model, Phase and Amplitude Impulse Sensitivity Functions (P-ISF and A-ISF respectively) are defined which relate circuit noise sources to the output phase and amplitude noises respectively. To obtain P-ISF and A-ISF, many simulations of the oscillator circuit at certain points and with certain parameters are needed [1], [2] which makes the method difficult to be performed. Some closed form expressions for P-ISF have been presented in [1], [3]–[5] which enable us to calculate the P-ISF only by one simulation. In [1], this analytical expression has been extracted from the limit cycle of the oscillator. In [3]–[5], based on the structure of the LC oscillators, some analytical expressions have been presented for P-ISF. However, the method in [1] is more general since it has been extracted from the limit cycle and therefore does not rely on the topology of the oscillator. While the phase noise has been calculated by the LTV model, there is no closed formula for A-ISF and no amplitude noise has been calculated by this model [6].

Recently, numerical models for the phase noise have been introduced which solve nonlinear differential equations of the oscillator circuit numerically by Harmonic Balance (HB) technique and calculate phase and amplitude noises and their correlation [7]–[11]. While these methods are accurate, some special and complicated computations are needed to evaluate the phase and amplitude noises which have not always been included in the commercial software.

In this paper, the amplitude and phase noises of electrical oscillators using the LTV model are investigated. For the first time, an analytical formula is derived for A-ISF based on the output limit cycle of the oscillator. So the calculation of this function can be easily performed only by one simulation. Since the extractions of P-ISF and A-ISF are derived from the limit cycle, they have the same origin and are correlated which is discussed in this paper. The behavior of the derived formula is investigated and the amplitude noise of electrical oscillators is calculated. Simulation and experimental results show the validity of the derived expressions and the evaluated amplitude and phase noises.

II. BRIEF REVIEW OF THE LTV MODEL

In a practical oscillator the output signal is [1]

$$V_{out}(t) = V_{\max}(t).\, f\left[\omega_0 t + \varphi(t)\right], \tag{1}$$

where $\varphi(t)$ and $A(t)$ are instantaneous phase and amplitude of the output respectively.

Consider an ideal and simplified model of a parallel LC oscillator shown in Fig. 1.

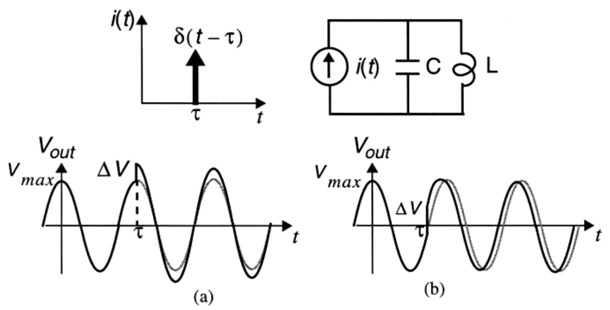

Fig. 1. Time domain response of an oscillator (a) impulse is injected at the peak (b) impulse is injected at the zero crossing point.

Based on the LTV model, if a current impulse is injected at time τ to the system, the instantaneous voltage change in the capacitor at the node i is [1]

$$\Delta vi = \frac{\Delta qi}{C_i}, \quad C_i = \frac{q_i}{v_i}, \tag{2}$$

Manuscript received January 20, 2012; accepted March 18, 2012.

where Δq_i is the total injected charge corresponding to the current impulse source and C_i is the total equivalent capacitance of the node i. For small injected charges, the phase change is [1]

$$\Delta\varphi = \Gamma(\omega_0 t)\frac{\Delta V_i}{V_i}, \tag{3}$$

where $\Gamma(\omega_0 t)$ is the phase impulse sensitivity function (P-ISF) which is a dimensionless, frequency- and amplitude-independent periodic function and describes the phase deviations for a unit impulse input at time τ. This phase change will be transformed into the output signal by the oscillator circuit and makes the phase noise.

In the 1/f^2 region of the phase noise spectrum, the resultant phase noise based on the LTV model is [1]

$$L(\Delta\omega) = 10\log\left(\frac{\Gamma_{RMS}^2}{q_{\max}^2}\cdot\frac{\overline{i_{noise}^2}/\Delta f}{2\Delta\omega^2}\right), \tag{4}$$

where Γ_{RMS} is the RMS value of P-ISF, $q_{\max}$ is the maximum charge on the node capacitor, $\overline{i_{noise}^2}/\Delta f$ is the white noise source spectral density in the oscillator circuit and $\Delta\omega$ is the offset frequency from the carrier.

The conventional method to calculate P-ISF is that an impulse current source is injected to the oscillator circuit at different phases of the oscillation period. Then the oscillator is simulated for a few cycles to reach the stable condition. This impulse causes a time shift ΔT in the output waveform. The excess phase for this time shift is $\Delta\varphi = 2\pi\Delta t/T$ where T is the period of oscillation. By sweeping the time in which the impulse is injected, different $\Delta\varphi$ and ΔV can be measured. Therefore $\Gamma(\omega_0 t)$ is calculated by (3).

Similar to the phase deviation, for small injected charges, the amplitude change is [2]

$$\Delta A = \Lambda(\omega_0 t)\frac{\Delta V_i}{V_i}, \tag{5}$$

where $\Lambda(\omega_0 t)$ is the amplitude impulse sensitivity function (A-ISF) which is a periodic function and describes the amplitude deviations for a unit impulse input at time τ. This amplitude change will be transformed into the output signal by oscillator circuit and makes the amplitude noise. Similar method to that of P-ISF is employed to calculate A-ISF [2].

In the 1/f^2 region of the spectrum, the resultant amplitude noise is [2]

$$L_{AM}\{\Delta\omega\} = \frac{\Lambda_{RMS}^2}{q_{\max}^2}\cdot\frac{\overline{i_{noise}^2}/\Delta f}{2\left(\frac{\omega_0^2}{Q^2}+\Delta\omega^2\right)}, \tag{6}$$

where Λ_{RMS} is the RMS value of A-ISF, ω_0 is the angular oscillation frequency and Q is the oscillator quality factor.

III. ANALYTICAL EXPRESSION FOR P-ISF

In [1], an analytical formula for P-ISF has been derived based on the output limit cycle. The extraction is brought here for simplicity.

For a stable oscillator, the limit cycle is defined as a closed trajectory in n-dimensional state space, where the state vector $\vec{X}$ traverses it once in every period of the oscillation, as shown in Fig. 2.

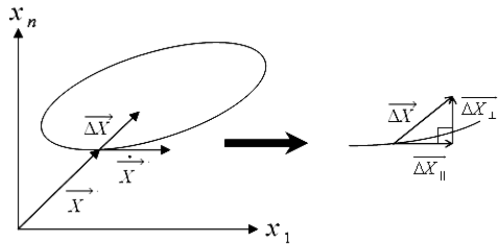

Fig. 2. Limit cycle of an oscillator.

Suppose that a perturbation vector $\overrightarrow{\Delta X}$, caused by circuit noise sources, changes the state of the system from $\vec{X}$ to $\vec{X}+\overrightarrow{\Delta X}$. This change in the state vector causes an equivalent displacement along the trajectory of the limit cycle. This displacement in turn makes a time shift which is related to the final phase shift. The unit tangential vector at the point of perturbation is

$$\overrightarrow{\Delta X_{\parallel}} = \frac{\dot{\vec{X}}}{||\dot{\vec{X}}||}. \tag{7}$$

The equivalent phase shift due to the perturbation vector is

$$\Delta\varphi = \frac{2\pi}{T}\cdot\frac{1}{||\dot{\vec{X}}||}\left(\overrightarrow{\Delta X}\cdot\overrightarrow{\Delta X_{||}}\right) = \frac{2\pi}{T}\cdot\frac{1}{||\dot{\vec{X}}||}\left(\overrightarrow{\Delta X}\cdot\frac{\dot{\vec{X}}}{||\dot{\vec{X}}||}\right), \tag{8}$$

where $\dot{\vec{X}}$ is the first derivative of the state vector with respect to time and $\|\cdot\|$ denotes the norm function. If the state variables are node voltages and an impulse is applied to the node i, there will be a change in ΔV_i given by (2). So (8) reduces to

$$\Delta\varphi_i = \frac{2\pi}{T}\cdot\frac{\Delta q_i}{C_i}\cdot\frac{\dot{V}_i}{||\dot{\vec{V}}||^2}. \tag{9}$$

Considering (9) with the normalized waveform function f defined in (1) results in

$$\Delta\varphi_i = \frac{\Delta V}{V_i}\cdot\frac{f_i'}{||\vec{f}'||^2}, \tag{10}$$

where $f' = \dot{f}/\omega_0$ and $\dot{f}$ is the derivative of the normalized waveform with respect to time on node i . Comparing (10) with (3) results in the following P-ISF

$$\Gamma_i(\omega_0 t) = \frac{f_i'}{\|\vec{f'}\|^2} = \frac{f_i'}{\sum_{j=1}^{n} f_j'^2}, \tag{11}$$

In the special case of the second order systems (which is a usual condition in practical oscillator circuits), (11) leads to the following expression for P-ISF [1]

$$\Gamma(\omega_0 t) = \frac{f'}{f'^2 + f''^2}, \tag{12}$$

IV. ANALYTICAL EXPRESSION FOR A-ISF

Here, we use the limit cycle of Fig. 2 and derive an analytical formula for the amplitude impulse sensitivity function (A-ISF). Since this formula is extracted from the limit cycle, any nonlinear behavior of the oscillator circuit will be included in A-ISF. Also in contrast to the conventional method which needs many simulations, using the formula only needs one simulation over one cycle of the oscillation to calculate A-ISF.

According to Fig 2, the perturbation vector $\overrightarrow{\Delta X}$ can be decomposed into its components: the tangential vector to the trajectory $\overrightarrow{\Delta X_{\parallel}}$ and the normal vector to the trajectory $\overrightarrow{\Delta X_{\perp}}$. For the normal vector, at the point of the perturbation we can write

$$\left|\overrightarrow{\Delta X_{\perp}}\right|^2 = \left|\overrightarrow{\Delta X}\right|^2 - \left|\overrightarrow{\Delta X}\,.\overrightarrow{\Delta X_{\parallel}}\right|^2, \tag{13}$$

where $\left|\overrightarrow{\Delta X_{\perp i}}\right|$ is equal to the amplitude deviation due to perturbations, i.e. ΔA_i at the node i . Substituting (7) in (13) results in

$$\left|\overrightarrow{\Delta X_{\perp}}\right| = \sqrt{\left|\overrightarrow{\Delta X}\right|^2 - \left(\frac{\overrightarrow{\Delta X}\cdot\vec{\dot{X}}}{\|\vec{\dot{X}}\|}\right)^2}. \tag{14}$$

If we consider node voltages as the state variables, for node i , we have

$$\Delta X_{\perp i} = \sqrt{\Delta V_i^2 - \left(\frac{\Delta V_i \cdot \dot{V}_i}{\|\vec{\dot{V}}\|}\right)^2} = \Delta V_i \sqrt{1 - \frac{\dot{V}_i^2}{\|\vec{\dot{V}}\|^2}}. \tag{15}$$

Normalizing (1) to $V_{i,\max}$ and considering (15) gives

$$\Delta X_{\perp i} = \frac{\Delta V_i}{V_{\max}} \sqrt{1 - \frac{\dot{f}_i^2}{\|\vec{\dot{f}}\|^2}}. \tag{16}$$

Comparing (16) with (5), we get

$$\Lambda_i(\omega_0 t) = \sqrt{1 - \frac{\dot{f}_i^2}{\|\vec{\dot{f}}\|^2}} = \sqrt{1 - \frac{f'^2_i}{\sum_{j=1}^{n} f_j'^2}}. \tag{17}$$

For second order systems, (17) reduces to

$$\Lambda(\omega_0 t) = \sqrt{1 - \frac{f'^2}{f'^2 + f''^2}}, \tag{18}$$

which represents the analytical expression for A-ISF.

Now, we show that P-ISF and A-ISF are correlated. Consider Fig. 2. The components $\overrightarrow{\Delta X_{\parallel}}$ and $\overrightarrow{\Delta X_{\perp}}$ of the perturbation vector $\overrightarrow{\Delta X}$ have the same origin and are correlated. Extraction of (12) shows that P-ISF corresponds to $\overrightarrow{\Delta X_{\parallel}}$. Also extraction of (18) shows that A-ISF corresponds to $\overrightarrow{\Delta X_{\perp}}$. Therefore P-ISF and A-ISF is correlated. Using (12) and (18), the relationship between P-ISF and A-ISF will be

$$\Lambda(\omega_0 t) = \sqrt{1 - f'.\Gamma(\omega_0 t)}. \tag{19}$$

V. SIMULATION RESULTS

To investigate the amplitude noise, two oscillator structures are considered. First, a Colpitts oscillator topology presented in [1] is proposed as in Fig. 3 with the given parameters for the transistor BFR520. With R=10kΩ, L=200nH, C1=40pF and C2=200pF, the oscillation frequency is 62MHz. For this oscillator, the output current, the output ac voltage (with dc value omitted) versus Radian and the A-ISF calculated by (18) are shown in Fig. 4a, Fig. 4b and Fig. 4c respectively.

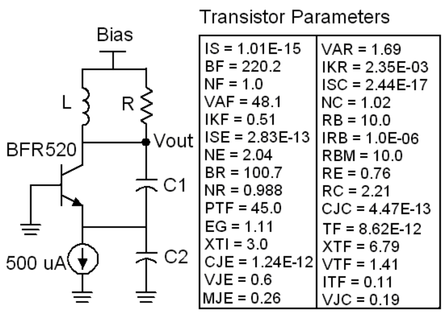

Fig. 3. The Colpitts oscillator.

To investigate the behavior of the calculated A-ISF, consider Fig. 1a. If an impulse is injected at the peak of the output signal, it makes the maximum amplitude deviation. If an impulse is injected at the zero crossing of the output, no amplitude deviation occurs as in Fig. 1b.

Considering Fig. 4b and Fig. 4c, applying an impulse at the positive or negative peak of the output voltage of the Colpitts oscillator (point A in Fig. 4b) causes maximum amplitude deviation at the output and consequently, at this point A-ISF must have maximum magnitude which is point A in Fig. 4c. Also, applying an impulse at zero crossing point (point B in Fig. 4b) causes no amplitude deviation at the output and consequently A-ISF must be zero at this point which is point B in Fig. 4c. This discussion shows that the behavior of A-ISF calculated by (18) is correct.

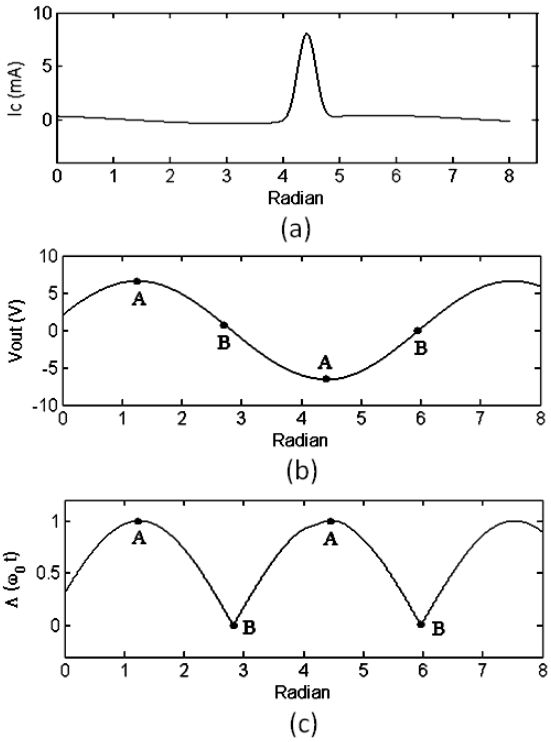

Fig. 4. (a) Transistor current (b) output voltage (c) A-ISF (Colpitts oscillator, R=10kΩ, L=200nH, C1=40pF, C2=200pF, f=62MHz).

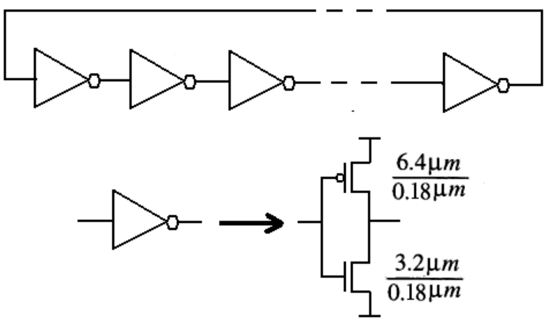

Fig. 5. Ring oscillator.

As another example a 19-stage ring oscillator (in TSMC 0.18µm technology) with oscillation frequency of 943 MHz is considered as in Fig. 5. The output current, the output ac voltage (with dc value omitted) versus Radian and the A-ISF calculated by (18) are shown in Fig. 6a, Fig. 6b and Fig. 6c respectively.

Similar to discussion for A-ISF behavior done for the Colpitts oscillator, applying an impulse at the positive or negative peak of the output voltage of the ring oscillator (point A in Fig. 6b) causes a maximum amplitude deviation at the output and consequently A-ISF at this point must have maximum magnitude which is point A in Fig. 6c).

Also applying an impulse at the zero crossing point B in Fig. 4b causes no amplitude deviation at the output and therefore A-ISF is zero at point B in Fig. 4c). This discussion shows that the behavior of A-ISF calculated by (18) is valid for this kind of oscillators.

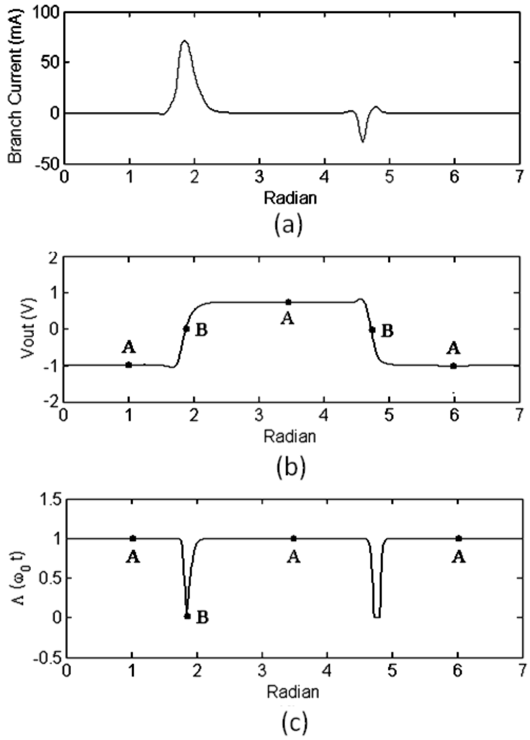

Fig. 6. (a) Branch current (b) output voltage (c) A-ISF (ring oscillator).

The transistor current of the Colpitts oscillator in Fig. 4a has a pulse shape and its magnitude is nearly zero during a part of the period. It modulates any stationary noise sources in the oscillator circuit (thermal noise of the resistor and shot noise of the transistor) and makes cyclostationary noise sources. In this case, new effective A-ISF will be introduced as [1]

$$\Lambda_{eff}(\omega_0 t) = \Lambda(\omega_0 t) \cdot \alpha(\omega_0 t), \tag{20}$$

where $\alpha(\omega_0 t)$ is a periodic function that describes the noise source modulation and can be calculated from the transistor current and is normalized to one [1]. The same situation exists for the current of the ring oscillator as in Fig. 6a.

Fig. 7 shows $\Lambda(\omega_0 t)$, $\alpha(\omega_0 t)$ and $\Lambda_{eff}(\omega_0 t)$ for the Colpitts oscillator. Fig. 8 shows $\Lambda(\omega_0 t)$, $\alpha(\omega_0 t)$ and $\Lambda_{eff}(\omega_0 t)$ for the ring oscillator. It is concluded from the figures that since the shape of the effective A-ISF is changed, the cyclostationary noise behavior has significant effects on amplitude noise and therefore must be always considered.

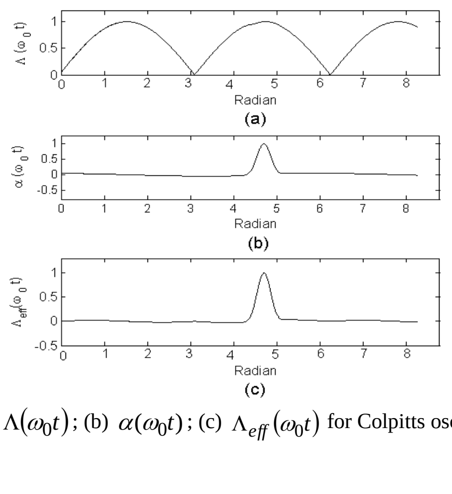

Fig. 7. (a) $\Lambda(\omega_0 t)$; (b) $\alpha(\omega_0 t)$; (c) $\Lambda_{eff}(\omega_0 t)$ for Colpitts oscillator.

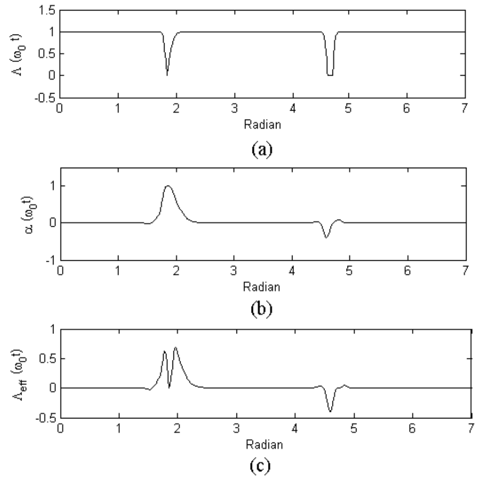

Fig. 8. (a) $\Lambda(\omega_0 t)$ (b) $\alpha(\omega_0 t)$ (c) $\Lambda_{eff}(\omega_0 t)$ for ring oscillator.

Now we calculate the amplitude noise of the Colpitts oscillator. In the $1/f^2$ region of the output noise spectrum, the total white noise power spectral density of the oscillator circuit is the shot noise of the transistor and the thermal noise of the resistor [1]

$$\frac{\overline{i_{noise}^2}}{\Delta f} = 2q_e I_C + \frac{4KT}{R}, \tag{21}$$

where q_e is the unit electron charge, T is the absolute temperature, k is the Boltzmann constant and I_C is the transistor dc current. Also Q can be approximated by $R\sqrt{\frac{C}{L}}$ for the LC oscillators where the variables are the resonator components. With R=10 kΩ, L=200nH, C1=40pF and C2=200pF, I_C=8mA and C_{total}=33.33pF. The maximum voltage swing is 8.14V. Therefore q_{max}=271.47 pC. Also Q=129, $\Lambda_{eff,RMS}$=0.22, and the noise power spectral density is 2.56×10^{-21} A^2/Hz.

Fig. 9 shows the amplitude noises calculated by (6) and by the Harmonic Balance (HB) method. Very good agreement can be inferred from the figure which can validate the derived expression of A-ISF.

Table I shows the amplitude noise for a Colpitts oscillator measured in [14] and calculated by (6). Good agreement for the results can be achieved from the table. The differences are for the colored noise sources.

TABLE I. AMPLITUDE NOISES MEASURED IN [14] AND CALCULATED BY (6).

Freq. (kHz)	100	300	800	1000
Measured [14]	-143.7	-144.6	-145.3	-145.5
Calculated (6)	-145.9	-146.5	-146.8	-147.0

Now we calculate the amplitude noise of the ring oscillator. For this oscillator, the quality factor is [12]

$$Q = \frac{3}{8}\sqrt{\frac{3N\pi \left| dV/dt \right|_{\max}}{\omega_0 V_{dd}}}, \tag{22}$$

where N is the numbers of stages and dV/dt is the derivative of the output voltage of the ring oscillator with respect to the time and ω_0 is the oscillation frequency.

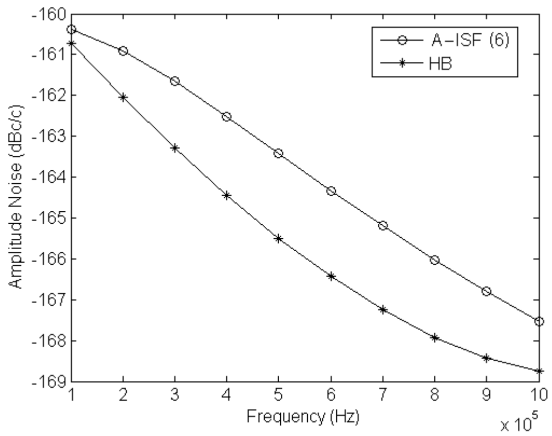

Fig. 9. Amplitude noises calculated by HB and (6) for Colpitts oscillator with R=10kΩ, L=200nH, C1=40pF, C2=200pF.

In the $1/f^2$ region of the output noise spectrum, the total white noise power spectral density for the ring oscillator circuit is the channel thermal noise which is [13]

$$\overline{I_{\text{Thermal}}^2} = 4kT\gamma\, g_m, \tag{23}$$

where T is the absolute temperature, k is the Boltzmann constant, γ is the thermal noise coefficient and is typically 2/3 for the MOSFETs. g_m is the transconductance of the transistor. g_m is measured at the middle of the output transition in which the output voltage changes from zero to maximum.

For the 19-stage ring oscillator, C_{total}=1.256pF and the maximum voltage swing is 1.8V. Therefore q_{max}=2.261pC. Also Q=8.1964, $\Lambda_{eff,RMS}$=0.0304. For PMOS g_m is 28.1 mS and for NMOS is 62.4 mS. So the noise power spectral density is 1.01×10^{-21} A^2/Hz. Fig. 10 shows amplitude noises calculated by (9) and the HB method. Very good agreement can be inferred from the figure which can validate the derived expression of A-ISF.

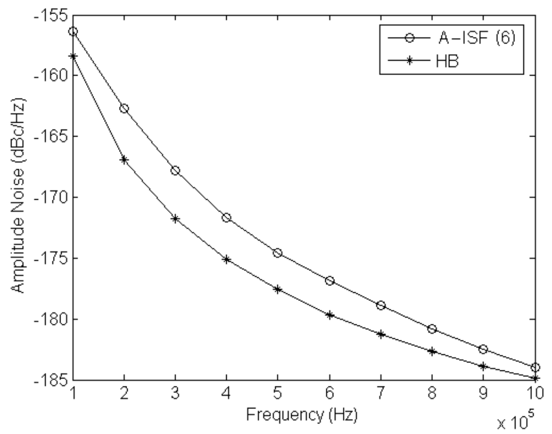

Fig. 10. Amplitude noises calculated by HB and (6) for 19-stage ring oscillator.

VI. CONCLUSIONS

In this paper, for the first time, an analytical expression was presented for the amplitude impulse response function (A-ISF) of the electrical oscillators. Also it was shown that the phase impulse response function, P-ISF, and A-ISF were correlated and their relationship was derived. Based on the derived A-ISF and the LTV model, amplitude noise of Colpitts and ring oscillators in the $1/f^2$ region of the noise spectrum were calculated.

REFERENCES

[1] A. Hajimiri, T. H. Lee, "A General Theory of Phase Noise in Electrical Oscillators", *Journal of Solid-State Circuits*, IEEE, vol. 33, pp. 179–194, 1998. [Online]. Available: http://dx.doi.org/10.1109/4.658619

[2] T. H. Lee, A. Hajimiri, "Oscillator Phase Noise: A Tutorial", *Journal of Solid-State Circuits*, IEEE, vol. 35, pp. 226–336, 2000.

[3] P. Andreani, X. Wang, L. Vandi, A. Fard, "A Study of Phase Noise in Colpitts and LC Tank CMOS Oscillators", *Journal of Solid-State Circuits*, IEEE, vol. 40, pp. 1107–1118, 2005. [Online]. Available: http://dx.doi.org/10.1109/JSSC.2005.845991

[4] P. Andreani, A. Fard, "More on the $1/f^2$ Phase Noise Performance of CMOS Differential Pair LC Tank Oscillators", *Journal of Solid-State Circuits*, IEEE, vol. 41, pp. 2703–2712, 2006. [Online]. Available: http://dx.doi.org/10.1109/JSSC.2006.884188

[5] A. Fard, P. Andreani, "An Analysis of $1/f^2$ Phase Noise in Bipolar Colpitts Oscillators (with a Digression on Bipolar Differential Pair LC Oscillators)", *Journal of Solid-State Circuits*, IEEE, vol. 42, pp. 374–384, 2007. [Online]. Available: http://dx.doi.org/10.1109/JSSC.2006.889388

[6] Murphy D., J. J. Rael, A. A. Abidi, "Phase Noise in LC Oscillators: A Phasor Based Analysis of a General Result and of Loaded Q", *Trans. On Circuits and Systems-I Regullar Papers*, IEEE, vol. 57, pp. 1187–1203, 2010.

[7] S. Jahanbakht, F. Farzaneh, "Computation of the Phase and Amplitude Noise in Microwave Oscillators and a Simplified Calculation Method for Far Enough From the Carrier Offsets", *IET Microwaves, Antennas & Propagation*, IET, vol. 4, pp. 2031–2041, 2010. [Online]. Available: http://dx.doi.org/10.1049/iet-map.2009.0396

[8] M. Ponton, E. Fernandez, A. Suarez, F. Ramirez, "Optimized Design of Pulsed Waveform Oscillators and Frequency Dividers", *Trans. On Microwave Theory and Techniques*, IEEE, vol. 59, pp. 3828–3440, 2011.

[9] H. Ghohnoodi, M. H. Naimi, "A Phase and Amplitude Tunable Quadrature LC Oscillator: Analysis and Design", *Trans. On Circuits and Systems-I Regullar Papers*, IEEE, vol. 58, pp. 677–689, 2011.

[10] M. Ponton, E. Fernandez, A. Suarez, F. Ramirez, "Analysis of Injection-Locked Pulsed Waveform Oscillators", in *Proc. of the 6th European Microwave Integrated Circuits Conference*, IEEE, vol. 2, 2011, pp. 156–159.

[11] S. Sancho, A. Suarez, J. Dominguez, F. Ramirez, "Analysis of Near-Carrier Phase-Noise Spectrum in Free-Running Oscillators in the Presence of White and Colored Noise Sources", *Trans. On Microwave Theory and Techniques*, IEEE, vol. 58, pp. 587–601, 2010.

[12] L. Dai, R. Harjani, "Design of Low Phase Noise Ring Oscillators", *Trans. On Circuit and Systems II: Digital Signal Processing*, IEEE, vol. 49, pp. 328–338, 2002.

[13] B. Razavi, *Design of Analog CMOS Integrated Circuits*, McGraw Hill, 2003.

[14] S. Sancho, A. Suarez, F. Ramirez, "Phase and Amplitude Noise Analysis in Microwave Oscillators Using Nodal Harmonic Balance" *Trans. On Microwave Theory and Techniques*, IEEE, vol. 55, pp. 1568–1583, 2007.